

Nonlinear dynamics of two coupled nano-electromechanical resonators

L. Chotorlishvili^{1,3}, A.Ugulava², G.Mchedlishvili², A. Komnik³, S. Wimberger³, J. Berakdar¹

1 Institut für Physik, Martin-Luther Universität, Halle-Wittenberg,

Heinrich-Damerow-Str. 4, 06120 Halle, Germany

2 Physics Department of the Tbilisi State University,

Chavchavadze av. 3, 0128, Tbilisi, Georgia

3 Institut für Theoretische Physik Universität Heidelberg,

Philosophenweg 19, 69120 Heidelberg, Germany

Abstract

As a model of coupled nano-electromechanical resonators we study two nonlinear driven oscillators with an arbitrary coupling strength between them. Analytical expressions are derived for the oscillation amplitudes as a function of the driving frequency and for the energy transfer rate between the two oscillators. The nonlinear restoring forces induce the expected nonlinear resonance structures in the amplitude-frequency characteristics with asymmetric resonance peaks. The corresponding multistable behavior is shown to be an efficient tool to control the energy transfer arising from the sensitive response to small changes in the driving frequency. Our results imply that the nonlinear response can be exploited to design precise sensors for mass or force detection experiments based on nano-electromechanical resonators.

PACS numbers:

I. INTRODUCTION

Currently experimental efforts are devoted to the fabrication of nanoscale resonators with a precise control of their behavior. Such nanoscale resonators are ideal prototype systems for testing fundamental physical concepts, such as entanglement and quantum correlations [1]. By now several types of resonators were successfully considered, like optical two level atoms in quantum cavities [2], artificial Josephson junction qubits [3], atoms seized in ion traps [4], or nano-optomechanical devices [5]. There is a new trend towards nano-electromechanical resonators. They are widely studied from both the quantum-mechanical [4, 6] and from a classical point of view [7–14]. These devices are approximately 200 nm in size and consist of three layers of gallium arsenide (GaAs): an n -doped layer of width 100 nm is stacked within an insulating layer of 50 nm and a p -doped layer of 50 nm [14]. The resonators can be controlled by electric fields via the piezoelectric effect, which fix their mechanical strain [13]. Along with a single resonator, one can consider coupled resonators driven by an additional external field. Coupled resonators show different dynamical regimes dependent on the interplay of their coupling strength and the driving. For the case of moderate coupling between two resonators this problem was already addressed in a recent paper by Karabalin *et al.* [14]. They showed that the linear and weakly nonlinear response of one oscillator can be modified by driving the second oscillator. A complicated frequency-sweep response curve was obtained numerically when both oscillators are driven into the strongly nonlinear regime.

In this paper we study two nonlinear oscillators allowing for an arbitrary coupling strength between them with a possibility of driving both with the same frequency but different amplitudes. The coupling strength between the oscillators is quantified in terms of the connectivity parameter defined below in Sect. II. We derive general analytical expressions for the amplitude-frequency characteristics valid for arbitrary (weak as well as strong) connectivity. We analyze the redistribution of energy between the two resonators injected into the system via the external driving fields. We quantify stable and unstable dynamical regimes, with special focus on the nonlinear response of the system. Our predictions point to possible new applications of nanoscale resonators exploiting their sensitivity in response to external fields and perturbations. In particular they may be used as sensors for tiny forces or masses [15, 16] which lead to a shift in their resonance frequencies to be identified in the sensitive

nonlinear response regime.

Our paper is organized as follows: in the next section, we discuss our fundamental model of two coupled driven oscillators. In Sect. III we study the mode frequency shifts and relaxation effects for a non-resonant driving, while in Sect. IV we address the resonant case with a special focus on the nonlinear shifts of the mode frequencies. In the following sections we investigate the frequency response function and the key problem of the energy redistribution between the oscillators, before concluding in Sect. VIII.

II. MODEL

We consider two nanomechanical oscillators described by the coordinates $x_{1,2}$ in the framework of the model outlined in [14]. The corresponding dynamical equations can be written down in the following form:

$$\begin{aligned}\ddot{x}_1 + \omega_1^2 x_1 + D(x_1 - x_2) &= \varepsilon M, \\ \ddot{x}_2 + \omega_2^2 x_2 + D(x_2 - x_1) &= \varepsilon N.\end{aligned}\tag{1}$$

$$\begin{aligned}\varepsilon M &= \varepsilon M(x_1, \dot{x}_1, t) = -2\gamma_1 \dot{x}_1 - \chi_1 x_1^3 + F_1 \cos \Omega t, \\ \varepsilon N &= \varepsilon N(x_2, \dot{x}_2, t) = -2\gamma_2 \dot{x}_2 - \chi_2 x_2^3 + F_2 \cos \Omega t,\end{aligned}\tag{1'}$$

$$\varepsilon \ll 1.$$

Here ω_1 and ω_2 are frequencies of the individual resonators, γ_1 and γ_2 are the dissipation coefficients, χ_1 and χ_2 are nonlinearity parameters, F_1 and F_2 are amplitudes of the external harmonic forces applied to the resonators, Ω is the frequency of these forces and D is the coefficient of the linear coupling between the resonators. As usual, we assume the right hand side of Eqs. (1) to be small perturbations, see also [14, 17–20].

We summarize the canonical solution of the unperturbed coupled system first. Its dynamics follows the simple equations

$$\begin{aligned}\ddot{x}_1 + \omega_1^2 x_1 + D(x_1 - x_2) &= 0, \\ \ddot{x}_2 + \omega_2^2 x_2 + D(x_2 - x_1) &= 0.\end{aligned}\tag{2}$$

The transition from coupled oscillations to the mode oscillations can be done via the following transformation [20],

$$x_1 = q_1 + q_2,$$

$$x_2 = -K^{-1}q_1 + Kq_2, \quad (3)$$

where

$$K = -\frac{1}{\sigma}(1 + \sqrt{1 + \sigma^2}), \quad K^{-1} = \frac{1}{\sigma}(1 - \sqrt{1 + \sigma^2}), \quad KK^{-1} = 1. \quad (4)$$

$$\sigma = \frac{2D}{|\omega_1^2 - \omega_2^2|}. \quad (5)$$

We call the parameter σ describing the coupling strength between the oscillators *connectivity*. From now on we assume that $\omega_2 > \omega_1$.

The mode oscillations have the frequencies

$$\nu_{1,2}^2 = \tilde{\omega}_+^2 \mp \omega_-^2 \sqrt{1 + \sigma^2}, \quad (6)$$

where

$$\begin{aligned} \tilde{\omega}_+^2 &= \frac{\tilde{\omega}_1^2 + \tilde{\omega}_2^2}{2}, \\ \tilde{\omega}_{1,2}^2 &= \omega_{1,2}^2 + D, \\ \omega_-^2 &= \frac{\omega_2^2 - \omega_1^2}{2}. \end{aligned} \quad (7)$$

$\tilde{\omega}_{1,2}$ are partial frequencies. We would like to stress that the value of the connectivity σ depends not only on the linear coupling term D , but on the proximity of the free oscillation frequencies ω_1 and ω_2 . In the limit of a weak connectivity ($\sigma \ll 1$) the frequencies $\nu_{1,2}$ tend to the partial frequencies $\tilde{\omega}_{1,2}$, while in the limit of strong connectivity ($\sigma \gg 1$),

$$\nu_1^2 \simeq \omega_+^2, \quad \nu_2^2 \simeq \tilde{\omega}_+^2, \quad (8)$$

where

$$\omega_+^2 = \frac{\omega_1^2 + \omega_2^2}{2}, \quad \tilde{\omega}_+^2 = \frac{\omega_1^2 + \omega_2^2}{2} + 2D.$$

Obviously, in the limit $\sigma \gg 1$ the mode frequency separation attains the maximal possible value which is equal to $2D$.

In the case of a finite driving $F_{1,2} \neq 0$ but in the linear ($\chi_{1,2} = 0$) dissipationless regime ($\gamma_{1,2} = 0$) the particular solutions of the dynamical equations (1) are given by

$$\begin{aligned} x_1 &= A_1 \cos \Omega t, \quad x_2 = A_2 \cos \Omega t, \\ A_{1,2} &= \frac{F_{1,2}(\tilde{\omega}_{2,1}^2 - \Omega^2) + F_{2,1}D}{d^2}, \end{aligned} \quad (9)$$

here

$$\begin{aligned} \frac{1}{d^2} &= \frac{1}{(\Omega^2 - \nu_1^2)(\Omega^2 - \nu_2^2)} = \\ &= \frac{1}{\Omega^2(\nu_2^2 - \nu_1^2)} \left(\frac{\nu_1^2}{\nu_1^2 - \Omega^2} - \frac{\nu_2^2}{\nu_2^2 - \Omega^2} \right) \end{aligned} \quad (10)$$

and $A_{1,2}$ are the amplitudes of the induced resonator oscillations. They increase resonantly when the frequency of the external driving tends closer to either of $\nu_{1,2}$.

With the above solutions at hand the influence of the damping term as well as of the nonlinear corrections can be taken into account with the help of a standard substitution in the resonant denominator [20]:

$$\begin{aligned} \frac{1}{\nu_{1,2}^2 - \Omega^2} &\rightarrow \frac{1}{2\nu_{1,2}(\nu_{1,2} - \Omega)} \rightarrow \frac{1}{2\nu_{1,2}(\nu_{1,2} + \delta_{1,2} + i\Gamma_{1,2} - \Omega)} \rightarrow \\ &\rightarrow \frac{1}{2\nu_{1,2}\sqrt{(\nu_{1,2} + \delta_{1,2} - \Omega)^2 + \Gamma_{1,2}^2}}, \end{aligned} \quad (11)$$

where $\Gamma_{1,2}$ are the mode relaxation rates, $\delta_{1,2}$ are the nonlinear corrections to the mode frequencies that depend on the oscillation amplitudes $A_{1,2}$. We would like to point out that the substitutions of Eq. (11) are correct only if the nonlinearity is not too strong and the decay rate is not too high ($\nu_{1,2} \gg \delta_{1,2}; \Gamma_{1,2}$). Explicit expressions for $\delta_{1,2}$ and $\Gamma_{1,2}$, in terms of the system parameters will be given in the next section.

III. NONLINEAR SHIFT OF THE MODE FREQUENCIES AND CONSEQUENCES OF THE RELAXATION TERMS. THE NON-RESONANT CASE

We turn back to the perturbed system of Eq. (1) making the preliminary assumption that the resonance condition does not hold at the mode frequencies $\nu_{1,2} \neq \Omega$. It is clear that in this particular case, the role of the external force is negligible. We concentrate at first on the influence of the relaxation and of the nonlinearity on the oscillation of the coupled resonators.

To study the equations (1), we use a modified method of a slowly varying amplitudes, [17]. Taking into consideration the transformation (3), we reduce the unperturbed system to the mode oscillations and write down the solution in the form:

$$x_1(t) = A_1(t) \sin[\nu_1 t + \alpha_1(t)] + A_2(t) \sin[\nu_2 t + \alpha_2(t)],$$

$$x_2(t) = -K^{-1}A_1(t) \sin[\nu_1 t + \alpha_1(t)] + KA_2(t) \sin[\nu_2 t + \alpha_2(t)], \quad (12)$$

where $A_{1,2}(t)$, $\alpha_{1,2}(t)$ are slowly varying amplitudes and phases, respectively. The variables $\dot{A}_{1,2}(t)$ are the first-order infinitesimal variables and therefore the terms proportional to the second-order derivatives $\ddot{A}_{1,2}(t)$ can be omitted upon an insertion of the above relations into Eq. (1). Following the standard procedures, after straightforward but laborious calculations, we find for the slowly varying amplitudes and the phases

$$\begin{aligned} \frac{dA_1}{dt} &= \frac{1}{4\nu_1} \frac{\sigma}{\sqrt{1+\sigma^2}} (-K^{-1}P_1 + Q_1), \\ \frac{dA_2}{dt} &= -\frac{1}{4\nu_2} \frac{\sigma}{\sqrt{1+\sigma^2}} (KP_2 + Q_2), \\ A_1 \frac{d\alpha_1}{dt} &= -\frac{1}{4\nu_1} \frac{\sigma}{\sqrt{1+\sigma^2}} (-K^{-1}P_3 + Q_3), \\ A_2 \frac{d\alpha_2}{dt} &= \frac{1}{4\nu_2} \frac{\sigma}{\sqrt{1+\sigma^2}} (KP_4 + Q_4), \end{aligned} \quad (13)$$

where

$$\begin{aligned} P_1 &= \frac{1}{4\pi^3} \int_0^{2\pi} \int_0^{2\pi} \int_0^{2\pi} M \cos \xi d\xi d\eta d\zeta, & Q_1 &= \frac{1}{4\pi^3} \int_0^{2\pi} \int_0^{2\pi} \int_0^{2\pi} N \cos \xi d\xi d\eta d\zeta, \\ P_2 &= \frac{1}{4\pi^3} \int_0^{2\pi} \int_0^{2\pi} \int_0^{2\pi} M \cos \eta d\xi d\eta d\zeta, & Q_2 &= \frac{1}{4\pi^3} \int_0^{2\pi} \int_0^{2\pi} \int_0^{2\pi} N \cos \eta d\xi d\eta d\zeta, \\ P_3 &= \frac{1}{4\pi^3} \int_0^{2\pi} \int_0^{2\pi} \int_0^{2\pi} M \sin \xi d\xi d\eta d\zeta, & Q_3 &= \frac{1}{4\pi^3} \int_0^{2\pi} \int_0^{2\pi} \int_0^{2\pi} N \sin \xi d\xi d\eta d\zeta, \\ P_4 &= \frac{1}{4\pi^3} \int_0^{2\pi} \int_0^{2\pi} \int_0^{2\pi} M \sin \eta d\xi d\eta d\zeta, & Q_4 &= \frac{1}{4\pi^3} \int_0^{2\pi} \int_0^{2\pi} \int_0^{2\pi} N \sin \eta d\xi d\eta d\zeta. \end{aligned} \quad (14)$$

For M and N , determined by Eq.(1'), after inserting $x_1(t)$ and $x_2(t)$ from (12), we obtain

$$\begin{aligned} M(\xi, \eta, \zeta) &= -\gamma_1(A_1\nu_1 \cos \xi + A_2\nu_2 \cos \eta + A_1\Omega \sin \zeta) - \alpha_1(A_1 \sin \xi + A_2 \sin \eta + A_1 \cos \zeta)^3, \\ N(\xi, \eta, \zeta) &= -\gamma_2(-A_1K^{-1}\nu_1 \cos \xi + A_2K\nu_2 \cos \eta - A_2\Omega \sin \zeta) - \\ &\quad -\alpha_2(-A_1K^{-1} \sin \xi + A_2K \sin \eta + A_2 \cos \zeta)^3, \\ \xi &= \nu_1 t + \alpha_1; \quad \eta = \nu_2 t + \alpha_2; \quad \zeta = \Omega t. \end{aligned} \quad (15)$$

Inserting (15) into (14), after simple integration, from (13) one infers

$$\frac{dA_1}{dt} = -\frac{1}{2}\Gamma_1; \quad \frac{dA_2}{dt} = -\frac{1}{2}\Gamma_2;$$

$$\frac{d\alpha_1}{dt} = \delta_1; \quad \frac{d\alpha_2}{dt} = \delta_2; \quad (16)$$

where

$$\begin{aligned} \Gamma_{1,2} &= \frac{1}{2} \left[\gamma_1 \left(1 \pm \frac{1}{\sqrt{1+\sigma^2}} \right) + \gamma_2 \left(1 \mp \frac{1}{\sqrt{1+\sigma^2}} \right) \right], \\ \delta_{1,2} &= \frac{3}{8} \cdot \frac{1}{\nu_{1,2}} \left[\chi_1 A_1^2 \left(1 \pm \frac{1}{\sqrt{1+\sigma^2}} \right) + \chi_2 A_2^2 \left(1 \mp \frac{1}{\sqrt{1+\sigma^2}} \right) \right] \end{aligned} \quad (17)$$

are the relaxation rates and the nonlinear shifts of the mode frequencies. An interesting fact is that the shift of the mode frequencies $\delta_{1,2}$ depends on the square of the amplitudes $A_{1,2}^2$ as a consequence of the nonlinearity.

In the case of a weak connectivity ($\sigma \ll 1$), from Eq. (17) we deduce

$$\Gamma_{1,2} \simeq \gamma_{1,2}, \quad \delta_{1,2} = \frac{3}{4} \frac{1}{\tilde{\omega}_{1,2}} \chi_{1,2} A_{1,2}^2,$$

while in case of strong connectivity ($\sigma \gg 1$)

$$\begin{aligned} \Gamma_1 = \Gamma_2 &\approx \frac{1}{2}(\gamma_1 + \gamma_2), \\ \delta_1 &\approx \frac{3}{8} \sqrt{\frac{2}{\omega_2^2 + \omega_1^2}} (\chi_1 A_1^2 + \chi_2 A_2^2), \\ \delta_2 &\approx \frac{3}{8} \sqrt{\frac{2}{\omega_2^2 + \omega_1^2 + 4D}} (\chi_1 A_1^2 + \chi_2 A_2^2). \end{aligned} \quad (18)$$

Therefore, when $\sigma \gg 1$ the modes are damped with the equal rates. However, the nonlinear shifts of the mode frequencies are different ($\delta_1 > \delta_2$).

IV. FREQUENCY RESPONSE FUNCTION OF TWO COUPLED RESONATORS

The amplitudes of the driven oscillations of the two coupled resonators are presented by the expressions (9) and (10). Reexpressed in terms of the connectivity σ , we can rewrite the amplitudes as

$$\begin{aligned} A_{1,2} &= \frac{F_{1,2}(\tilde{\omega}_{2,1}^2 - \Omega^2) + F_{2,1}\omega_-^2\sigma}{2\Omega^2} \times \\ &\times \left[\frac{\omega_+^2}{\omega_-^2} \frac{1}{\sqrt{1+\sigma^2}} \left(\frac{1}{\nu_1^2 - \Omega^2} - \frac{1}{\nu_2^2 - \Omega^2} \right) - \left(\frac{1}{\nu_1^2 - \Omega^2} + \frac{1}{\nu_2^2 - \Omega^2} \right) \right]. \end{aligned} \quad (19)$$

In the limit of a weak connectivity ($\sigma \ll 1$) $A_{1,2} = 2F_{1,2}/(\omega_{1,2}^2 - \Omega^2)$ whereas in the limit of a strong connectivity ($\sigma \gg 1$) we obtain

$$A_{1,2} = \frac{DF_{2,1}}{\Omega^2} \left(\frac{1}{\Omega^2 - \omega_+^2} + \frac{1}{\Omega^2 - \tilde{\omega}_+^2} \right). \quad (20)$$

Nanomechanical resonators for intermediate values of the connectivity ($\sigma \approx 2$) were studied numerically and experimentally in [14]. While the general analytical expression (19) is derived for arbitrary values of the connectivity and therefore in the special case of a moderate connectivity the solution recovers the amplitude-frequency characteristics obtained in [14]. Using the transformation (11), one can easily modify (19) in order to add corrections describing the damping and nonlinear terms. However, the expressions obtained in this way are rather involved (see Appendix A). That is why here we only present the asymptotic expressions corresponding to the strong connectivity limit ($\sigma \gg 1$):

$$A_{1,2} \simeq \frac{DF_{1,2}}{\Omega^2} \left(\frac{1}{\omega_+ \sqrt{(\omega_+ + \delta_1 - \Omega)^2 + \Gamma_1^2}} + \frac{1}{\tilde{\omega}_+ \sqrt{(\tilde{\omega}_+ + \delta_2 - \Omega)^2 + \Gamma_2^2}} \right), \quad (21)$$

where $\delta_{1,2}$ and $\Gamma_{1,2}$ are determined in (18).

As follows from (21), in the case of a strong connectivity the force F_2 acting on the second oscillator, “drives” the first one, and vice versa – F_1 , acting on the first oscillator, “drives” the second one.

The amplitude–frequency characteristic consists of two tilted peaks with different heights, see Fig. 1. The first peak corresponds to the frequency ω_+ and is definitely more pronounced than the second peak, corresponding to the frequency $\tilde{\omega}_+$ ($\tilde{\omega}_+ \gg \omega_+$). Furthermore, the first peak is more tilted due to the relation $\delta_1 > \delta_2$. The parts of the plot CD and IH , corresponding to unstable oscillations of the system, are dotted. During upward/downward frequency sweeps of Ω one observes hysteretic behaviour around $\Delta\omega_+$ and $\Delta\tilde{\omega}_+$ along the loops $-BCED$ and $GIKH$, respectively.[17, 20] In [14] similar hysteretic loops in amplitude–frequency characteristics of coupled nonlinear oscillators were obtained numerically and were confirmed experimentally for intermediate values of the connectivity $\sigma \approx 2$. In the unstable region the system is extremely sensitive to the perturbations. This fact can be used for the switching of the oscillation amplitude. After reaching the point C , the amplitude of the oscillation decreases sharply to the value E . Therefore, a simple and efficient switching protocol can be realized by tuning of the external field frequency only.

We would like to point out, that the domain of the amplitude frequency characteristics that should be utilized for switching belongs to the unstable area (see the frequency intervals $B - C$ and $G - I$ on Fig. 1). Therefore, the system can jump to the lower state before reaching the summit of the unstable domain (point C). If this happens the jump of the oscillation amplitude is smaller making difficult the experimental observation of the two different

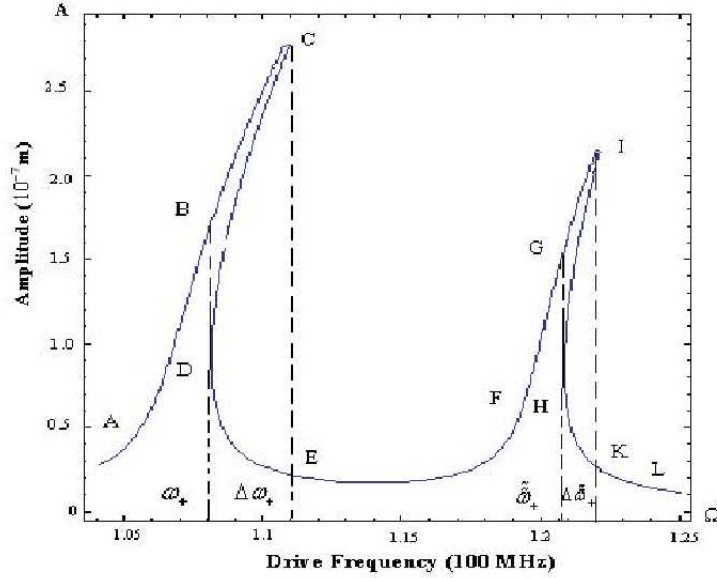


FIG. 1: Amplitude-frequency characteristics for the system of two strongly coupled oscillators, plotted using Eq.(21) and following values of the parameters: $F_1 = F_2$, $A = A_{1,2}$, $\omega_+ = 1.07 \cdot 10^8 \text{ Hz}$, $\tilde{\omega}_+ = 1.2 \cdot 10^8 \text{ Hz}$, $\delta_1 = 50.4 \cdot 10^{18} A^2 \text{ Hz}$, $\delta_2 = 45.0 \cdot 10^{18} A^2 \text{ Hz}$, $\Gamma_1 = \Gamma_2 = 2.0 \cdot 10^5 \text{ Hz}$, $DF_{1,2} = 81.6 \cdot 10^{21} mHz^4$.

transport regimes. To circumvent this problem the frequency of the driving field should be changed adiabatically. Following our approach here we seek the criteria of adiabaticity that may be useful for different realizations of the system. A similar problem arises for example when studying nonlinear resonant transport in cold atoms [21]. The method of the slow varying amplitudes implies that the amplitude change rate should be slower than the mode frequencies $\nu_{1,2}$. Therefore, the rate of the oscillation amplitude change caused by tuning the frequency of the driving field is limited by the following condition:

$$\frac{dA_{1,2}(\Omega(t))}{dt} = \frac{dA_{1,2}(\Omega(t))}{d\Omega(t)} \frac{d\Omega(t)}{dt} < \nu_{1,2} A_{1,2}(\Omega(t)). \quad (22)$$

The adiabaticity condition can then be simplified taking into account the explicit expressions for the amplitudes given in Eq. (21). It is not difficult to show that in the vicinity of unstable areas

$$\frac{dA_{1,2}(\Omega(t))}{d\Omega(t)} \approx \frac{2A_{1,2}(\Omega(t))}{\Omega(t)}. \quad (23)$$

Thus, for the adiabaticity criteria we finally obtain the following estimation

$$\frac{d\Omega(t)}{dt} < \min(\nu_{1,2}) \frac{\Omega(t)}{2}. \quad (24)$$

V. NONLINEAR SHIFT OF THE MODE FREQUENCIES AND THE INFLUENCE OF THE RELAXATION TERMS. THE RESONANT CASE

Let us suppose that the harmonic force $F_1 \cos \Omega t$ is tuned in resonance with one of the modes and that $F_2 = 0$. For this problem we derive equations for the slowly varying amplitudes in a more straightforward way. Taking into consideration the resonance condition and the transformation (3), we can write down the solution of the equation set (1) in the following form:

$$\begin{aligned} x_1(t) &= A_1(t) \sin \nu_1 t + A_2(t) \cos \nu_1 t + B(t) \sin(\nu_2 t + \psi(t)), \\ x_2(t) &= -K^{-1}(A_1(t) \sin \nu_1 t + A_2(t) \cos \nu_1 t + KB(t) \sin(\nu_2 t + \psi(t))). \end{aligned} \quad (25)$$

After application of the standard method outlined in the last Section, for equations of slowly varying amplitudes and phases we obtain

$$\begin{aligned} \frac{dA_1}{dt} &= \frac{1}{4\nu_1} \frac{\sigma}{\sqrt{1+\sigma^2}} (-K^{-1}P_1^{(r)} + Q_1^{(r)}), \\ \frac{dA_2}{dt} &= -\frac{1}{4\nu_1} \frac{\sigma}{\sqrt{1+\sigma^2}} (-KP_2^{(r)} + Q_2^{(r)}), \\ \frac{dB}{dt} &= -\frac{1}{4\nu_2} \frac{\sigma}{\sqrt{1+\sigma^2}} (K^{-1}P_3^{(r)} + Q_3^{(r)}), \\ \frac{1}{B} \frac{d\psi}{dt} &= \frac{1}{4\nu_2} \frac{\sigma}{\sqrt{1+\sigma^2}} (KP_4^{(r)} + Q_4^{(r)}), \end{aligned} \quad (26)$$

where

$$\begin{aligned} P_1^{(r)} &= \frac{1}{2\pi^2} \int_0^{2\pi} \int_0^{2\pi} M \cos \eta d\xi d\eta, & Q_1^{(r)} &= \frac{1}{2\pi^2} \int_0^{2\pi} \int_0^{2\pi} N \cos \eta d\xi d\eta, \\ P_2^{(r)} &= \frac{1}{2\pi^2} \int_0^{2\pi} \int_0^{2\pi} M \sin \eta d\xi d\eta, & Q_2^{(r)} &= \frac{1}{2\pi^2} \int_0^{2\pi} \int_0^{2\pi} N \sin \eta d\xi d\eta, \\ P_3^{(r)} &= \frac{1}{2\pi^2} \int_0^{2\pi} \int_0^{2\pi} M \cos \xi d\xi d\eta, & Q_3^{(r)} &= \frac{1}{2\pi^2} \int_0^{2\pi} \int_0^{2\pi} N \cos \xi d\xi d\eta, \\ P_4^{(r)} &= \frac{1}{2\pi^2} \int_0^{2\pi} \int_0^{2\pi} M \sin \xi d\xi d\eta, & Q_4^{(r)} &= \frac{1}{2\pi^2} \int_0^{2\pi} \int_0^{2\pi} N \sin \xi d\xi d\eta. \end{aligned} \quad (27)$$

$$\xi = \nu_2 t + \psi, \quad \eta = \Omega t,$$

$$\begin{aligned} M^{(r)} &= M^{(r)}(x_1, \dot{x}_1, t) = -\gamma_1 [\nu_1 (A_1 \cos \eta - \sin \eta) + B \cos \xi] - \\ &\quad - \chi_1 (A_1 \sin \eta + A_2 \cos \eta + B \cos \xi)^3 + F \cos \Omega t, \end{aligned}$$

$$N^{(r)} = N^{(r)}(x_2, \dot{x}_2, t) = -\gamma_2 [-K^{-1}\nu_1 (A_1 \cos \eta - A_2 \sin \eta) + \nu_2 B \cos \xi] -$$

$$- \chi_2[-K^{-1}(A_1 \sin \eta + A_2 \cos \eta) + KB \sin \xi]^3. \quad (28)$$

Upon insertion of Eqs.(28) into (27) and after an integration, one gets equations for the slowly varying amplitudes A_1, A_2, B and ψ . The explicit form of these equations is given in Appendix B. In the limit of a strong connectivity ($\sigma \gg 1$), the expressions simplify to

$$\begin{aligned} \frac{dA_1}{dt} &= \frac{F}{4\Omega} - \gamma A_1 - \frac{3\chi}{8\Omega}(A_1^2 + A_2^2 + 2B^2)A_2, \\ \frac{dA_2}{dt} &= -\gamma A_2 + \frac{3\chi}{8\Omega}(A_1^2 + A_2^2 + 2B^2)A_1, \\ \frac{dB}{dt} &= -\gamma B. \end{aligned} \quad (29)$$

As is evident, a resonant external force $F_1 \cos \Omega t$, ($\Omega = \nu_1$), for $\gamma = \chi = 0$ leads to the simplest form of instability (the secular instability), namely to the linear growth of the oscillation amplitude $A_1 = (F/4\Omega)t$.

We would like to point out that in the first three equations for the variables A_1, A_2 and B , the right hand side of the set of Eqs. (29) does not depend on the fourth variable ψ . Therefore, the set of Eqs. (29) can be solved self-consistently for the first three variables.

In order to find the stationary values of the slowly varying amplitudes and in order to examine the stability of these values, we utilize the following transformation:

$$A_1 = \rho \cos \theta, \quad A_2 = -\rho \sin \theta. \quad (30)$$

In the more convenient polar coordinates ρ and θ we obtain

$$\begin{aligned} \frac{d\rho}{dt} &= -\gamma\rho + \frac{F}{4\Omega} \cos \theta, \\ \frac{d\theta}{dt} &= -\omega_{NL} - \frac{F}{4\Omega} \frac{\sin \theta}{\rho}, \\ \frac{dB}{dt} &= -\gamma B, \end{aligned} \quad (31)$$

where $\omega_{NL} = \frac{3\chi}{8\Omega}(\rho^2 + 2B)$. By setting the rhs of Eqs. (31) equal to zero, we obtain equations for the stationary values of amplitudes:

$$B_0 = 0, \quad s \cos \theta_0 = \rho_0, \quad s \sin \theta_0 = -r\rho_0^3, \quad (32)$$

where $s = \frac{F}{4\gamma\Omega}$, $r = \frac{3}{4} \frac{\chi}{\gamma\Omega}$. To determine ρ_0 , we eliminate the variable θ_0 from the set of Eqs. (31) and obtain a cubic equation with respect to $x = \rho_0^2$:

$$x^3 + \frac{x}{r^2} - \frac{s^2}{r^2} = 0. \quad (33)$$

Eq. (33) is a reduced cubic equation. The number of real roots of this equation depends on the sign of the discriminant:

$$D = \left(\frac{1}{3r^2}\right)^3 + \left(\frac{s^2}{2r^2}\right)^2 > 0, \quad (34)$$

which is positive in our case. That is why Eq. (33) has a real root. Real roots of Eq. (33) can be identified easily with the help of well-known Cardano's formula [22]. However, as it will become evident below, they are not necessary for a further specification of the expressions for the stationary points need for the study of the stability conditions.

To address the question concerning the stability of the stationary points more precisely we linearize the set of Eqs. (29) in the vicinity of the stationary points $A_1^{(0)} = \rho_0 \cos \theta_0$, $A_2^{(0)} = \rho_0 \sin \theta_0$ and $B_0 = 0$, and obtain:

$$\begin{aligned} \delta \dot{A}_1 &= -\gamma(1 + 2rA_1^{(0)}A_2^{(0)})\delta A_1 - \gamma r(A_1^{(0)2} + 3A_2^{(0)2})\delta A_2, \\ \delta \dot{A}_2 &= \gamma r(A_2^{(0)2} + 3A_1^{(0)2})\delta A_1 - \gamma(1 - 2rA_1^{(0)}A_2^{(0)})\delta A_2. \end{aligned} \quad (35)$$

Alternatively, by taking into consideration the transformation (30):

$$\begin{aligned} \delta \dot{A}_1 &= R_{11}\delta A_1 + R_{12}\delta A_2, \\ \delta \dot{A}_2 &= R_{21}\delta A_1 + R_{22}\delta A_2, \end{aligned} \quad (36)$$

where

$$R = \begin{pmatrix} -\gamma(1 + r\rho_0^2 \sin 2\theta_0) & -\gamma r\rho_0^2(3 - \cos 2\theta_0) \\ \gamma r\rho_0^2(3 + \cos 2\theta_0) & -\gamma(1 - r\rho_0^2 \sin 2\theta_0) \end{pmatrix}. \quad (37)$$

As discussed in [18], the type of the stability is determined by three characteristics of the matrix (R):

$$T = R_{11} + R_{22}, \quad d = R_{11}R_{22} - R_{12}R_{21}, \quad T^2 - 4d. \quad (38)$$

With the help of the matrix (R), it is easy to check, that in our case the characteristics of the matrix $\|R\|$ are

$$T = -2\gamma < 0, \quad d = \gamma^2(1 + 8r^2\rho_0^4) > 0, \quad T^2 - 4d = 32\gamma^2r^2\rho_0^2 > 0 \quad (39)$$

and point towards the condition of a stable focus. Note, that the conditions (39) do not depend on the field parameter $s = \frac{F}{4\gamma\Omega}$, and therefore hold for arbitrary values of the amplitudes (A_1 , A_2).

Thus, in the stationary resonance regime, when frequency of the external driving field is in the resonance with one of the modes of the two strongly coupled resonators, the stationary points are characterized by a stable focus. Therefore, we can argue that the dissipation leads to a stabilization of the secular instability regime.

VI. ENERGY REDISTRIBUTION BETWEEN RESONATORS

In this section we will address the problem of the energy redistribution between the resonators (A_1^2/A_2^2) , which are pumped via the external fields. Let us suppose that the harmonic force acts only on the second resonator $F_2 \equiv F$, $F_1 = 0$. Then, with the help of the expression (10), for the ratio of the oscillation amplitudes we obtain the following relation:

$$\left| \frac{A_1}{A_2} \right| = \frac{D}{\tilde{\omega}_1^2 - \Omega^2}. \quad (40)$$

We recall that the expressions (10) for the amplitudes $A_{1,2}$ with respect to the mode frequencies $\nu_{1,2}$ have the same resonances embedded in the denominators. They naturally compensate each other and therefore do not appear in the ratio A_1/A_2 . Nevertheless, as we see from Eq. (40), another resonance $\tilde{\omega}_1 \approx \Omega$ appears in the denominator of the expression A_1/A_2 .

At first we neglect the influence of the damping and the nonlinearity terms, assuming that the frequency of the harmonic force is tuned with one of the partial frequencies of the resonators. Then for the case when $F_2 \equiv F$, $\Omega \simeq \tilde{\omega}_2$ and $F_1 = 0$, we obtain

$$\left| \frac{A_1}{A_2} \right| = \frac{D}{|\tilde{\omega}_1^2 - \tilde{\omega}_2^2|} \approx \frac{\sigma}{2}. \quad (41)$$

Hence, the relation between the amplitudes A_1 and A_2 is linear. From the second resonator a fraction $\frac{\sigma^2}{4}$ of the energy is transferred to the first one. The damping and the nonlinear corrections can be considered again with the help of the substitution:

$$\frac{1}{\tilde{\omega}_1^2 - \Omega^2} \rightarrow \frac{1}{2\tilde{\omega}_1 \sqrt{(\beta A_1^2 - \Delta)^2 + \gamma^2}}, \quad \beta = \frac{3}{4} \frac{\chi}{\omega_1}. \quad (42)$$

From now on we assume that

$$\gamma_1 \simeq \gamma_2 \equiv \gamma, \quad \chi_1 = \chi_2 = \chi \quad \text{and} \quad \Delta = \omega_2 - \omega_1 > 0.$$

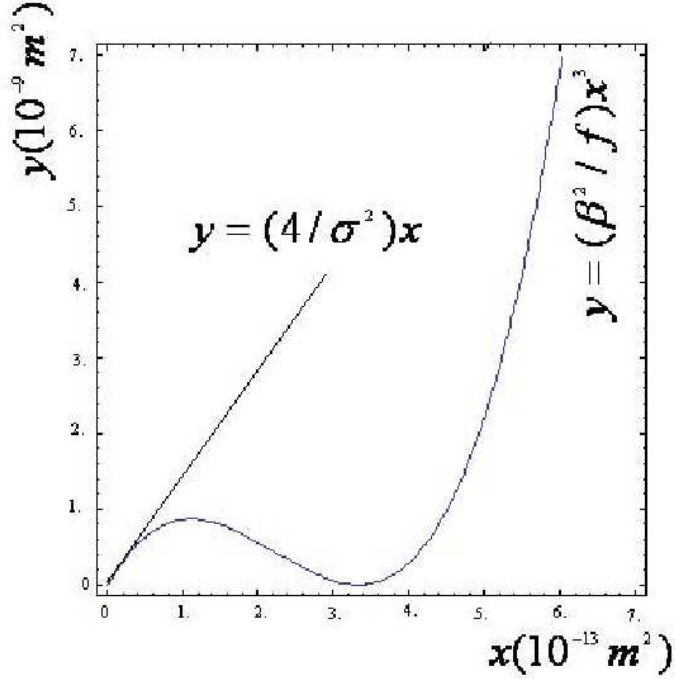


FIG. 2: Energy redistribution curve between the coupled resonators and its asymptotics, plotted using Eq. (44) for the following values of parameter $\beta = 0.51 \cdot 10^{20} \text{ Hz/m}$, $\Delta = 0.17 \cdot 10^8 \text{ Hz}$, $\gamma = 2.0 \cdot 10^5 \text{ Hz}$, $f = 1.64 \cdot 10^{10} \text{ Hz}^2$.

The resonant denominator is an important feature of the expression (42). When A_1 changes the resonance condition holds in the expression (42). Performing the substitution (42) in the expression (40) and raising to the square, we obtain

$$\frac{x}{y} = \frac{f}{(\beta x - \Delta)^2 + \gamma^2}, \quad (43)$$

where $x = A_1^2$, $y = A_2^2$, $f = \frac{D^2}{4\omega^2}$. So, instead of studying the dependence $y = Y(x)$, for convenience one can convert the problem to one studying the following implicit function

$$F(x, y) = x[(\beta x - \Delta)^2 + \gamma^2] - fy = 0. \quad (44)$$

By setting the derivative dy/dx equal to zero, one obtains an equation for the extrema of the function $y = Y(x)$

$$\frac{dy}{dx} = -\frac{dF/dx}{dF/dy} = f^{-1}(3\beta^2 x^2 - 4\beta x\Delta + \Delta^2 + \gamma^2) = 0. \quad (45)$$

It follows then that the points of extremum are

$$x_{1,2} = \frac{2\Delta}{3\beta} \left(1 \pm \sqrt{1 - \frac{3\Delta^2 + \gamma^2}{4\Delta^2}} \right). \quad (46)$$

For simplicity, we consider the limiting case $\gamma \ll \Delta$. In this case we get two real roots from Eq. (46):

$$x_1 = \frac{\Delta}{\beta}, \quad x_2 = \frac{\Delta}{3\beta}. \quad (47)$$

It is easy to determine the signs of the second derivatives:

$$\left. \frac{d^2 y}{dx^2} \right|_{x=x_1} = \frac{2\beta\Delta}{f} > 0, \quad \left. \frac{d^2 y}{dx^2} \right|_{x=x_2} = -\frac{2\beta\Delta}{f} < 0. \quad (48)$$

Therefore, the function $y = Y(x)$ has a maximum at the point $x = x_2$, and a minimum at $x = x_1$. The curve $y = Y(x)$ is characterized by two asymptotes as well. The first one, for small values of x and y , is a linear function $y = (\Delta^2/f)x = (4/\sigma^2)x$. The second one, for large values of x and y , is a cubic function $y = (\frac{\beta^2}{f})x^3$. Using the results obtained in this section, one can plot the curve of the energy redistribution between the resonators, see Fig. 2.

The anharmonicity of resonators' oscillations can significantly change the energy redistribution between the resonators. It turns out, that the energy pumped into the second resonator via the external energy source $F_2 = F$ is transformed to the first resonator ($F_1 = 0$) in a different way depending on the oscillations amplitude. For small amplitudes of the normal modes, the energy transfer between the resonators is linear, $A_1^2 = \frac{\sigma}{4}A_2^2$ and the transfer rate is defined by the values of the connectivity σ . With increasing oscillation amplitude the linear law is changed and turns nonlinear $A_1^2 = \left(\frac{4}{9} \cdot \frac{D^2}{\chi^2} A_2^2\right)^{1/3}$. Therefore, we can conclude that the anharmonicity of the oscillations degrades the energy transfer rate.

VII. APPLICATION TO MASS MEASUREMENT SENSORS AND THE NON-LINEAR SHIFT OF THE MODE FREQUENCIES

Nanomechanical resonators can be used as apprehensible sensors in many applications. For a review see [23]. A decisive advantage of the nanomechanical resonators are their resonance frequencies $\omega \approx 1GHz$ and quality factors $Q \approx 10^3 - 10^5$, which are significantly higher than those of electrical resonant circuits. That is the reason why nanomechanical resonators are sensitive transducers for the detection of molecular systems, in particular for biological molecules [16]. Resonant mass sensor devices operate by measuring the frequency shift which is proportional to the mass of the molecules of the material under investigation [24]. Details of the measurement protocol can be found in [25]. Here we briefly refer to the

main facts. Assuming that the added mass δM is smaller than the effective resonator mass M one can write a linearized expression $\delta M \approx \frac{\partial M}{\partial \omega} \delta \omega$. The minimal measurable frequency shift $\delta \omega$ naturally defines the sensitivity of the sensor. Due to thermal fluctuations $\delta \omega > 0$. For the single, simple damped harmonic oscillator system the minimal measurable frequency shift reads [25]

$$\delta \omega \approx \left[\frac{k_B T}{M \omega^2 A^2} \frac{\omega \Delta f}{Q} \right]^{1/2}. \quad (49)$$

Here Δf is the measurement bandwidth, M is the resonator mass, ω is the frequency of the oscillation and T is the temperature. As follows from the analysis of the preceding sections, at low temperatures the nonlinear effects (that were not considered in [25]) can produce a frequency shift larger than the minimum measurable frequency shift associated with the thermal effects (see Eq. (18)) $\delta_{1,2} > \omega_{1,2}$. We propose to use the system of coupled nonlinear oscillators to act as an amplifier for the frequency shifts. We are convinced that in this way far better mass measurements are possible for experiments described in [25].

VIII. CONCLUSION

We have developed a general analytical treatment of a system of two coupled driven nonlinear nanomechanical resonators, which is valid for an arbitrary coupling strength (connectivity) between them. We derive general analytical expressions for the amplitude–frequency characteristics of the system with a special emphasis on the energy redistribution and the energy transport between the resonators. The obtained results are valid for arbitrary values of the connectivity. In the limit of a weak coupling one recovers the previously obtained results [14]. In particular we have shown that the amplitude–frequency characteristic consists of two tilted peaks, the frequency separation between which is equal to twice the value of the resonators coupling constant $2D$. If the frequency of the external force Ω is swept the oscillation amplitude shows two hysteresis loops in the vicinity of the mode frequencies. These hysteresis loops contain unstable areas, in which a slight change of the driving frequency is accompanied by an instantaneous and a significant change of the oscillation amplitude. This is an interesting phenomenon, since it can be utilized to switch easily between the energy transport regimes of the resonators. We found that for small oscillation amplitudes the energy transfer between the resonators follows a linear law $A_1^2 = \frac{\sigma}{4} A_2^2$ and the transfer rate is entirely defined by the values of the connectivity σ . With increasing the oscillation

amplitude the energy transfer law turns nonlinear $A_1^2 = \left(\frac{4}{9} \cdot \frac{D^2}{\chi^2} A_2^2\right)^{1/3}$ and therefore the transport rate becomes slower. Switching off the energy transfer rate by tuning of the driving field frequency is a simple protocol from an experimental point of view and therefore we expect it to be easily observable.

Acknowledgments: The financial support by the Deutsche Forschungsgemeinschaft (DFG) through SFB 762, contract BE 2161/5-1, Grant No. KO-2235/3, the HGSFP (grant number GSC 129/1), the Heidelberg Center for Quantum Dynamics and STCU Grant No. 5053 is gratefully acknowledged.

Appendix A – details from section IV

By taking into account damping effects, the amplitudes of the forced oscillation of the nonlinear resonators for an arbitrary value of the connectivity σ are:

$$A_{1,2} = \frac{F_{1,2}(\tilde{\omega}_{2,1}^2 - \Omega^2) + F_{2,1}\omega_-^2\sigma}{4\Omega^2} \cdot \left[\frac{\omega_+^2}{\omega_-^2} \frac{1}{\sqrt{1+\sigma^2}} \left(\frac{1}{\nu_1\sqrt{(\nu_1+\delta_1-\Omega)^2+\Gamma_1}} - \frac{1}{\nu_2\sqrt{(\nu_2+\delta_2-\Omega)^2+\Gamma_2}} \right) - \left(\frac{1}{\nu_1\sqrt{(\nu_1+\delta_1-\Omega)^2+\Gamma_1}} + \frac{1}{\nu_2\sqrt{(\nu_2+\delta_2-\Omega)^2+\Gamma_2}} \right) \right].$$

Appendix B – details from section V

The explicit form of the set of equations

$$\begin{aligned} \frac{dA_1}{dt} &= \frac{1}{4\Omega} \frac{(1+\sqrt{1+\sigma^2})}{\sqrt{1+\sigma^2}} F_1 - \frac{1}{2} \frac{1}{\sqrt{1+\sigma^2}} \left[\gamma_1(1+\sqrt{1+\sigma^2})A_1 + \gamma_2(-1+\sqrt{1+\sigma^2})A_1 \right] - \\ &\quad - \frac{1}{4\Omega} \frac{1}{\sqrt{1+\sigma^2}} \left[\frac{3}{4}\chi_1(1+\sqrt{1+\sigma^2})(A_1^2 + A_2^2 + 2B^2)A_2 + \frac{3}{4}\chi_2(-1+\sqrt{1+\sigma^2}) \times \right. \\ &\quad \left. \times \left(\frac{\sigma^2}{(1+\sqrt{1+\sigma^2})^2} (A_1^2 + A_2^2) + \frac{\sigma^2}{(1-\sqrt{1+\sigma^2})^2} 2B^2 \right) A_2 \right], \\ \frac{dA_2}{dt} &= -\frac{1}{2} \frac{1}{\sqrt{1+\sigma^2}} \left[\gamma_1(1+\sqrt{1+\sigma^2})A_2 + \gamma_2(-1+\sqrt{1+\sigma^2})A_2 \right] + \end{aligned}$$

$$\begin{aligned}
& + \frac{1}{4\Omega} \frac{1}{\sqrt{1+\sigma^2}} \left[\frac{3}{4} \chi_1 (1 + \sqrt{1+\sigma^2}) (A_1^2 + A_2^2 + 2B^2) A_1 + \right. \\
& \left. + \frac{3}{4} \chi_2 (-1 + \sqrt{1+\sigma^2}) \left(\frac{\sigma^2}{(1 + \sqrt{1+\sigma^2})^2} (A_1^2 + A_2^2) + \frac{\sigma^2}{(1 - \sqrt{1+\sigma^2})^2} 2B^2 \right) A_1 \right],
\end{aligned}$$

$$\frac{dB}{dt} = -\frac{1}{4} \left(\frac{-1 + \sqrt{-1 + \sigma^2}}{\sqrt{1 + \sigma^2}} \gamma_1 + \frac{1 + \sqrt{1 + \sigma^2}}{\sqrt{1 + \sigma^2}} \gamma_2 \right) B,$$

$$\begin{aligned}
\frac{d\psi}{dt} = \frac{3}{16\nu_2} \cdot & \left[\frac{\sigma}{\sqrt{1 + \sigma^2}} \frac{\sigma}{1 + \sqrt{1 + \sigma^2}} (2A_1^2 + 2A_2^2 + B^2) \chi_1 + \right. \\
& \left. + \frac{(1 + \sqrt{1 + \sigma^2})}{\sigma} \left(\frac{(1 + \sqrt{1 + \sigma^2})^2}{\sigma^2} B^2 + 2 \frac{(1 - \sqrt{1 + \sigma^2})^2}{\sigma^2} (A_1^2 + A_2^2) \right) \chi_2 \right].
\end{aligned}$$

- [1] J. Raimond, M. Brune, S. Haroche, Rev. Mod. Phys. **73**, 565 (2001).
- [2] D. Bruss and G. Leuchs, Lectures on Quantum Information, Wiley VCH Verlag, Weinheim (2007).
- [3] S.N. Shevchenko, S. Ashhab, F. Nori, Phys. Rep. **492**, 1 (2010).
- [4] D. Leibfried, R. Blatt, C. Monroe, and D. Wineland, Rev. Mod. Phys. **75**, 281 (2003).
- [5] F. Marquardt and S. M. Girvin, Physics **2**, 40 (2009); L. Ding, Ch. Baker, P. Senellart, A. Lemaitre, S. Ducci, G. Leo, and I. Favero, Phys. Rev. Lett. **105**, 263903 (2010); M. Ludwig, K. Hammerer, and F. Marquardt Phys. Rev. A **82**, 012333 (2010); G. Heinrich and F. Marquardt, Europhys. Lett. **93**, 18003 (2011).
- [6] T. J. Harvey, D. A. Rodrigues, and A. D. Armour, Phys. Rev. B **81**, 104514 (2010).
- [7] R. Lifshitz and M.C. Cross, Reviews of Nonlinear dynamics and Complexity, edited by H.G.Shuster (Wiley, Weinheim, 2008), Chap.1, p.52.
- [8] R. Lifshitz and M.C. Cross, Phys. Rev. B **67**, 134302 (2003).
- [9] Y. Bromberg, and R. Lifshitz, Phys.Rev.E **73**, 016214 (2006).
- [10] H.G. Craighead, Science **290**, 1532 (2000).
- [11] E. Buks and M.L. Roukes, Europhys. Lett. **54**, 220 (2001).
- [12] D. Rugar and P. Grutter, Phys. Rev. Lett. **67**, 699 (1991).

- [13] C. Masmanidis et al., *Science* **317**, 780 (2007).
- [14] R.B. Karabalin, M.C. Cross and M.L. Roukes, *Phys.Rev. B* **79**, 165309 (2009).
- [15] M. L. Roukes, Technical Digest of the 2000 Solid-State Sensor and Actuator Workshop (2000), cond-mat/0008187.
- [16] L.M. Fischer et al *Sensors and Actuators B* **134**, 613 (2008).
- [17] A. Blaquiere, *Nonlinear System Analysis* (Academic Press New York and London) (1966).
- [18] N. Hand and J.D. Finch, *Analytical Mechanics*, Cambridge Univ. Press, Cambridge, 1998.
- [19] Steven H. Strogatz, *Nonlinear Dynamics and Chaos*, Addison-Wesley, Reading MA, 1994.
- [20] L.D. Landau and E.M. Lifshitz, *Mechanics (Course of Theoretical Physics) vol.1*, 3ed., Pergamon (1976).
- [21] T. Paul, K. Richter, and P. Schlagheck, *Phys. Rev. Lett.* **94**, 020404 (2005).
- [22] G. A. Korn and T. M. Korn, *Mathematical Handbook for Scientists and Engineers*. McGraw-Hill, New York (1961).
- [23] K. Brueckner et al., *Phys. Status Solidi A* **208**, 357 (2011).
- [24] B. Ilic, Y. Yang, and H. G. Craighead, *Appl. Phys. Lett.* **85**, 2604 (2004).
- [25] K. L. Ekinici, Y. T. Yang and M. L. Roukesb, *J. Appl. Phys.* **95**, 2682 (2004).